Published in final edited form as:
J Cell Physiol. 2012 July ; 227(7): 2880–2888. doi:10.1002/jcp.23032.

Initiation of BMP2 Signaling in Domains on the Plasma Membrane

Jeremy Bonor[1,□], **Elizabeth L. Adams**[1,2,□], **Beth Bragdon**[1,3], **Oleksandra Moseychuk**[1], **Kirk J. Czymmek**[1,2], and **Anja Nohe**[1,*]

[1]Department of Biological Sciences, University of Delaware, Newark, DE, 19716, USA

[2]Delaware Biotechnology Institute, University of Delaware, Newark, DE, 19716, USA

[3]Department of Biomedical Sciences, University of Maine, Orono, ME, 04469 USA

Abstract

Bone Morphogenetic Protein 2 (BMP2) is a potent growth factor crucial for cell fate determination. It directs the differentiation of mesenchymal stem cells into osteoblasts, chondrocytes, adipocytes and myocytes. Initiation of BMP2 signaling pathways occurs at the cell surface through type I and type II serine/threonine kinases housed in specific membrane domains such as caveolae enriched in the caveolin-1 beta isoform (CAV1β, caveolae) and clathrin coated pits (CCPs). In order for BMP2 to initiate Smad signaling it must bind to its receptors on the plasma membrane resulting in the phosphorylation of the BMP type Ia receptor (BMPRIa) followed by activation of Smad signaling. The current model suggests that the canonical BMP signaling pathway, Smad, occurs in CCPs. However, several recent studies suggested Smad signaling may occur outside of CCPs. Here we determined; 1) The location of BMP2 binding to receptors localized in caveolae, CCPs or outside of these domains using AFM and confocal microscopy. 2) The location of phosphorylation of BMPRIa on the plasma membrane using membrane fractionation, and 3) The effect of down regulation of caveolae on Smad signaling. Our data indicates that BMP2 binds with highest force to BMP receptors localized in caveolae. BMPRIa is phosphorylated in caveolae and the disruption of caveolae inhibited Smad signaling in the presence of BMP2. This suggests caveolae are necessary for the initiation of Smad signaling. We propose an extension of the current model of BMP2 signaling, in which the initiation of Smad signaling is mediated by BMP receptors in caveolae.

Keywords

BMP receptor; Confocal; AFM; Force volume measurement

Introduction

Embryonic development and tissue homeostasis are dependent upon stem cell fate and differentiation. For stem cells to properly differentiate they must receive both extracellular and intracellular signals. BMP2 is one of the earliest and most effective growth factors to designate cellular fate during embryogenesis. BMP2 signals through BMP receptors (BMPRs), type I and type II serine/threonine kinase receptors. In particular the BMPR type Ia (BMPRIa) and BMPR type II (BMPRII) are expressed in various tissues (Bragdon et al.,

[*]To whom correspondence should be addressed at Department of Biological Sciences, University of Delaware, Newark, DE, 19716, USA, Phone: (302) 831-2959, Fax: (302) 831-2281, anjanohe@udel.edu.
[□]Both authors contributed equally

2011; Ide et al., 1998; Yanai et al., 2005). Once BMP2 binds to its receptors, BMPRII phosphorylates and activates BMPRIa. Activated BMPRIa initiates several downstream signaling pathways including the BMP2 canonical pathway Smad, and others such as p38 Map kinase, NFkB, JNK, PI-3K and ERK 1/2 (Gamell et al., 2008; Itoh et al., 2000; Mukai et al., 2007; Pachori et al., 2010; Reilly et al., 2005; Sieber et al., 2009; Yamashita et al., 1996).

Although BMPRIa and BMPRII are segregated and colocalize to caveolae, clathrin coated pits (CCPs) and outside of these domains on the plasma membrane (Bragdon et al., 2009; Hartung et al., 2006; Jiang et al., 2011; Nohe et al., 2004; Nohe et al., 2003; Nohe et al., 2005; Ramos et al., 2006; Wertz and Bauer, 2008), the current model proposes that Smad signaling is activated in CCPs (Hartung et al., 2006). Caveolae are flask-shaped invaginations of the cell membrane enriched with cholesterol and Caveolin-1 (CAV1). There are two isoforms of CAV1, CAV1α and CAV1β (Fujimoto et al., 2000; Kogo and Fujimoto, 2000; Ramirez et al., 2002). CCPs are sites of classical coated pit endocytosis and receptor recycling where the membrane is coated with Clathrin, Dynamin, and adapter proteins including Adaptor protein 2 (AP2) (McNiven, 1998; Mellman, 1996; Schmid, 1997). However, this signaling model does not include recent findings. Several recent studies suggested Smad signaling may occur outside of CCPs (Bragdon et al., 2009; Chen et al., 2007; Murphy, 2007; Rauch et al., 2002; Shi et al., 2007; Wertz and Bauer, 2008). Using Atomic Force Microscopy (AFM) combined with confocal microscopy, we showed that BMP2 binds with highest force to BMP receptors localized in caveolae. Membrane fractionation showed BMPRIa is phosphorylated in caveolae. Additionally, reporter gene assays showed that disruption of caveolae did not induce Smad signaling in the presence of BMP2, suggesting caveolae are necessary for the initiation of Smad signaling. We propose an extension of the current model of BMP2 signaling that the initiation of Smad signaling is mediated by BMP receptors in caveolae.

MATERIALS AND METHODS

Materials

Recombinant BMP2 was obtained from GenScript (Piscataway, NJ). The cell line C2C12 was purchased from American Type Culture Collection (Manassas, VA). Monoclonal mouse anti-phospho-serine (p-Ser) antibody and G-sepharose were purchased from Invitrogen (Camarillo, CA). Polyclonal goat anti-sera against BMPRIa, horseradish peroxidase (HRP) conjugated goat anti-donkey IgG, goat anti-mouse IgG-HRP, siRNA against CAV1 and BMPRIa were purchased from Santa Cruz Biotechnology (Santa Cruz, CA). Monoclonal mouse anti-CAV1 was purchased from BD Transduction Laboratories (San Jose, CA).

Cell culture

Murine myoblast cells (C2C12) were grown in Dulbecco's Modified Eagle's Medium (Hy-Clone, Pittsburgh, PA) supplemented with 10% (v/v) fetal bovine serum (FBS) (Gemini Bio Products, West Sacramento, CA), 0.5% (v/v) L-Glutamine (Cellgro, Manassas, VA) and 1% (v/v) penicillin/streptomycin (Hy-Clone, Pittsburgh, PA).

Transfection of C2C12 cells

Cells were transfected with Turbofect from Fermentas Inc. (Glen Burnie, MD) using manufacture's protocol. One μg of plasmid for imaging, two μg of plasmid for reporter gene assays, and 20 ρmole or 80 ρmole of the siRNA (Santa Cruz Biotechnology, Santa Cruz, CA) against BMPRIa or CAV1 was used for transfections.

Functionalizing AFM Tip

The AFM probes (Bruker Probes and NanoWorld, nominal spring constant of 0.06–0.08 N/m, August-Schanz-Straβe) were silanized (4% 3-amino-propyltrimethylethoxysilane (3-APTES)) in 95% ethanol solution for one hour at room temperature. Surfaces were activated using 2.5% glutaraldehyde solution, followed by incubation with BMP2 (500nM, GenScript, Piscataway, NJ). Functionalized AFM probes stored in PBS at 4°C until use.

Confocal-AFM setup

Images were collected by incorporating an inverted laser scanning confocal microscope (Zeiss LSM 510 NLO) with an AFM (Bruker Inc, Bioscope II AFM, August-Schanz-Straβe). The process to set up the instrument and collect the data involved alignment and calibration of the instruments following integration. The maximum load was set below Bueckle's indentation depth limit of 10% of the specimen thickness (Buckle, 1973; Persch et al., 1994). For the C2C12 cells the maximum load was set to 21 nN or 230 nm. . When all the settings were aligned and tested, the data for a specific region of the cell was collected by using the Force volume setting at ramp speed (4um/s tip velocity), scan rate of 14.0 Hz, samples/line 16 at 16 lines resulting in 256 data points collected. This data was then extracted and tested for binding evens, which gave us the binding interaction that have occurred out of the 256 events collected. Image registration was performed using microscopy image registration overlay (MIRO) canvas software on the Bruker Bioscope II AFM in order to align the movements of the AFM stage with the Zeiss LSM 510 confocal image so that any movement in tip position matched the confocal field of view. The number of binding events typically ranged from 80–190 with associated binding forces of 0.1 to 1 nN. The cell membrane was expected to be relatively flat, so it would be anticipated that there would be an absence of large peaks or valleys within the scanned AFM area. After registration, fine tuning of tip position was performed.

Data was collected from regions of the membrane, away from the cell nucleus, using the AFM force volume parameters (16×16 image with a scan size of 4.49 μm) immediately followed by confocal microscope imaging. Confocal images (512×512) were acquired using a Zeiss 100×Plan-Apochromat objective lens (numerical aperture 1.4) and 488 nm argon laser excitation with 500–550 nm band pass emission filter. The closed loop scanner made it possible to collect data from the area defined by the MIRO software. Force and topographical data were also simultaneous collected.

The data was screened during and after data collection, using the following criteria: data was rejected if; (1) the AFM tip drifted off the cell during data collection, (2) the cell detached from the substrate causing movement of the cell under the scanning AFM tip (ranging from slight movement of membrane regions to complete detachment of the cell.) (3) Tip contamination resulting in very high or very low number of binding events, (4) If the agreement was not good between the AFM height image and the confocal image of the cell membrane, and, (5) Overexpression of caveolin-1 beta was shown to inhibit BMP2 signaling (Nohe et al., 2005). Therefore we ensured to select cells not significantly overexpressing caveolin-1 beta by choosing cells with low intensity.

After data passed the validation steps the images from both the AFM and the confocal (collected after the AFM image) were both imported into the Reconstruct software (Release: 1.1.0.0). To take into account any cellular movement the AFM images were then warped to match the confocal image as closely as possible. These aligned images were then imported into Corel Photo-Paint. After the overlay alignment of the image sets, the resulting stack of images was then cropped to the AFM data region using Corel Photo-Paint. The cropped

region was then enlarged 300%, using the resample tool, and the dpi were increased by the same 300% resulting in an image of workable size.

Confocal-AFM Data analysis

Once equipment setup and calibrations were completed, regions of the cell were then selected for force volume analysis. In each case a threshold force value was used to help determine the presence or absence of the specific regions in plasma membranes. Analysis of the force volume data sets revealed approximately 80–190 force curves containing detectable binding forces out of the total 256 force curves collected per data set (forces ranged from 0.1 and 1.0 nN). An overlay was then created and used as a reference to map the confocal data from the live cell. The binding forces were matched with the confocal image collected using this overlay. For the confocal image a z-stack was collected after the force volume mapping and the optical slice representing the upper membrane was used in the analysis. Only a limited number of caveolae vesicles are known to be present in the cytoplasm at room temperature and movement of the domains on the cell surface are very slow ($\approx 0.9 \pm 0.2 * 10^{-12}$ cm^2/sec^{-1}) About 5–10% of caveolae are immobile (Keating et al., 2008).

Sucrose Density Gradients

Sucrose density gradients were performed by modifying the procedure (Song et al., 1996). C2C12 cells were grown to 90% confluency in large flasks and serum starved for 24 hours before stimulation. Cells were then stimulated or not stimulated with 40nM BMP2 for 0 or 30 minutes and lysed using 3 ml of 1% Triton X-100 lysis buffer (1% Triton X-100, 1mM EDTA pH7.4, 10mM Tris pH7.4) in the presence of 1mM PMSF, 1mM DTT, 10mM tetrasodium pyrophosphate, 17.5mM β-glucrophosphate and protease inhibitor mix (1mg/ml of each of Leupeptin, Aprotinin, Soybean Trypsin inhibitor, Benzamidine/ HCl, Pepstatin, and Antipain), followed by pulse sonication. Three milliliters of sample were then mixed with 3 mL of 90% sucrose solution in Mes-Buffered saline (25mM Mes pH 6.5, 0.15M NaCl), placed at the bottom of the ultracentrifuge tubes, and overlaid with 3 mL 35% Sucrose Mes-Buffered Saline (0.25M Na2CO3). Three milliliters of 5% sucrose in Mes-Buffered saline containing 0.25M Na2CO3 was then placed on the top of the tube discontinuous sucrose gradient. Tubes were placed in Beckman swinging bucket rotor (SW41Ti) and spun at 39000rpm for 18 hours at 4°C in Beckman L8-55M ultracentrifuge. One milliliter fractions were collected from the top of the gradient followed by trichloroacetic acid (TCA) precipitation (precipitated with 20% v/v TCA, centrifuged, and washed with acetone). BMPRIa was immunoprecipitated as described in (Bragdon et al., 2010). Samples were put in 5× SDS running buffer and run on SDS PAGE gel. Western blotting was performed using a CAV1 antibody, BMPRIa antibody, or p-Ser antibody. Western blot was detected by enhanced chemiluminescence (ECL) (Pierce).

Reporter Gene Assays

Reporter gene assays were performed as described in (Bragdon et al., 2010) with the exception CAV1 was knocked down. Cells were treated with 5nM Nystatin to disrupt caveolae (Matveev et al., 2001). Luciferase activity was measured using a Firefly & Renilla Luciferase Assay Kit from Biotium (Hayward, CA).

Statistical Analysis

Experiments were performed three independent times or 5 independent cells for the confocal-AFM experiments. Values of the standard error of the mean (SEM) were calculated from the raw data at the 95% confidence level and was used for error bars on graphs. Significance was established with ANOVA followed by Tukey test or student t test as

indicated. Data for reporter gene assays are presented as a normalized value which is the value divided by control values.

RESULTS

Development of a biologically active BMP2-coated AFM tip

AFM combined with confocal microscopy was applied to determine the location of BMP2 binding to its receptors on the plasma membrane in live cells. AFM is a powerful tool that can be used to study ligand-receptor interactions. By combining AFM with confocal microscopy ligand-receptor interactions on the plasma membrane of live cells can be quantified (Doak et al., 2008; Haupt et al., 2006; Muller et al., 2009).

First, a functional BMP2-coated AFM tip was developed by covalently linking BMP2 to the AFM tip as described in materials and methods. This tip was used to quantify the binding force and location of BMP2 interactions with the plasma membrane. Force volume measurements of BMP2 interactions with the cell surface were determined on at least three different cells using an AFM. The specificity of BMP2 binding was verified by measuring the binding forces and events of an uncoated and a BMP2 coated AFM tip.

Figure 1A shows 23 binding events per cell. This was measured using the non-coated AFM tip. The binding events were significantly increased to 78 using the BMP2 functionalized AFM tip. When soluble BMP2 was added to block BMP2 binding sites on the plasma membrane, the number of binding events with the BMP2-coated AFM tips decreased to 60 (Figure 1B). The binding curves were collected at one location on five cells, resulted in a range of binding forces. The non-coated AFM tip binding force with the cell surface of live C2C12 cells was 0.013 nN. The binding forces for the BMP2-coated AFM tips significantly increased to 0.157 nN (Fig 1C). Addition of soluble BMP2 (133 nM) to the dish reduced the average binding force of the BMP2-coated tip to 0.09 nN (Figure 1D).

As another control BSA was coated to the AFM tip. Binding of BSA to the cell surface revealed a random binding pattern with an average force of 0.2 nN and 139 binding events per cell, demonstrating unspecific binding at the cell surface (Figure 1A and 1C). These results verified that BMP2 is able to interact with the cell surface when functionalized to an AFM tip.

BMP2 binding and force volume is increased in caveolae

With our newly functionalized AFM tip we investigated the location of BMP2 interaction with the plasma membrane using combined confocal-AFM. C2C12 cells were transfected with plasmids encoding CAV1β, provided by Hiroshi Kogo, (Department of Anatomy, Nagoya University School of Medicine, Nagoya, Japan) and AP2, obtained from Dr. Steve Furguson, (Roberts Research Institute, London, ON, Canada) fused to green fluorescent protein (GFP). These proteins were used to visualize caveolae and CCPs, respectively. Additionally, to validate the results of BMP2 binding forces, cells were co-transfected with siRNA against CAV1 or BMPRIa resulting in protein knockdown as described by manufacturing protocol. Combined confocal-AFM was applied to determine the binding forces for BMP2-BMPRIa interactions mapped to caveolae, CCPs, and regions independent of these domains (areas not fluorescently marked) in live cells. Briefly, the alignment procedure for confocal and AFM used three points as shown in Figure 2A–C. The AFM tip position was then fine-tuned (Figure 2D), data was collected from the area of the cell surface and exported (Figure 2E and 2F). The number of binding events typically ranged from 80–190 with associated binding forces of 0.1 to 1 nN. The cell membrane was expected to be relatively flat (Figure 2F), so it would be anticipated that there would be an absence of large peaks or valleys within the scanned AFM area. After registration, fine tuning of tip position

was performed AFM and confocal images were collected. Representative images and binding curves that were collected are shown in Figure 3. An overlay was then created to be used as a reference to map the confocal data from the live cell (Figure 4). The binding forces were matched with the confocal image collected using the overlay (Supplementary Table 1).

The data shown in Figure 5A, the binding force of BMP2 (0.335 nN), was significantly increased in caveolae enriched CAV1β regions compared to the CAV1β independent regions (0.2 nN). Knockdown of CAV1β using siRNA showed a significant reduction in the binding force of BMP2 (0.21nN) and binding events (60) compared to total binding events (130). Knockdown was achieved as shown in Figure 5E. The knockdown of BMPRIa reduced the total number of binding events from 130 to 78 (20 ρmoles siRNA BMPRIa) and 61 (80 ρmoles siRNA BMPRIa) (Figure 5B).

To investigate the binding of BMP2 to CCPs the binding force associated with CCPs was collected from C2C12 cells transfected with a plasmid encoding AP2 GFP as a marker. The results in Figure 5C showed a significant decrease in the BMP2 binding force in CCPs (0.15nN) compared to outside AP2 (0.23nN).

Phosphorylated BMPRIa is associated with caveolae

Once BMP2 binds to BMPRIa and BMPRII, the BMPRII activates BMPRIa by phosphorylation. Since BMP2 interacts with BMPRIa localized in caveolae, the phosphorylation state of BMPRIa in caveolae was determined using membrane fractionation. C2C12 cells were stimulated with 40 nM BMP2 for 0 or 30 minutes. Lysates were subjected to continuous and discontinuous sucrose density gradient as described in the materials and methods. After ultracentrifugation fractions were collected from the top of the gradient and were immunoprecipitated for BMPRIa. Samples were subjected to SDS-PAGE followed by detection for p-Ser as a marker of phosphorylated BMPRIa (p-BMPRIa). To determine the fractions containing CAV1, marker for caveolae, cells were lysed at 0 minutes BMP2 stimulation and subjected to sucrose gradient. After fractions were applied to SDS-PAGE followed by Western blotting for CAV1, caveolae were detected in fractions 3–5 (Figure 6). Under non-stimulated conditions, the BMPRIa bands were detected in fractions 3–8 with trace amounts of p-BMPRIa identified in the CAV1 associated fraction 4. Addition of BMP2 increased p-BMPRIa in fractions 4 and 5; both fractions are associated with CAV1. Markers for clathrin coated pits, Golgi, Endoplasmic reticulum (ER), and early endosomes are detected in dense fractions (Cai et al., 2008; Shin et al., 2000). For here it would be fractions 8, 9 and 10. BMPRIa phosphorylation was also detected in other fractions. There was no change with the total BMPRIa distribution after BMP2 stimulation; bands were located in fractions 3–10.

Caveolae regulate BMP2-induced Smad signaling

Downstream of the phosphorylation of BMPRIa is the activation of the Smad-1, -5, and -8 pathway. These Smads complex with Smad 4 and translocate to the nucleus where gene transcription is regulated (Itoh et al., 2000). Since our results obtained from the combined confocal AFM experiments and BMPRIa immunoprecipitation and phosphorylation experiment suggested caveolae were the centers for the initiation of BMP2 signaling we defined the role caveolae has on the genetic level of Smad signaling. C2C12 cells were transfected with plasmids encoding pSBE (Smad binding element fused with firefly luciferase), and pRLU (renilla luciferase used for normalization). Caveolae were disrupted by transfection with siRNA against CAV1 or treated with Nystatin (5nM). Cells were stimulated with 40 nM BMP2 or non-stimulated (control). Treatment with BMP2 induced a significant 2.6 fold increase in Smad signaling compared to the control (Figure 7). When caveolae were disrupted by the knockdown of CAV1 or Nystatin treatment, the BMP2

stimulation did not result in a significant Smad signal. The reporter gene assay using the pSBE was recently shown to correlate with Smad phosphorylation in C2C12 cells (Jiang et al., 2011).

DISCUSSION

Our data showed that caveolae are the centers for the initiation of BMP2 signaling, BMP2 interacts with BMPRIa, and BMPRIa is phosphorylated. Further caveolae regulate Smad signaling. Therefore the current model of Smad signaling must be extended. Combination of confocal microscopy and AFM allowed us to measure the interactions between BMP2 and its receptors by quantifying the number of binding events and forces on live cells. We determined that BMP2 was able to interact with and bind to its receptors at the cell surface when attached to an AFM tip by measuring a range of different binding forces. Additionally, our results using correlative approach demonstrated that BMP2 bound with a higher affinity to BMPRIa localized to domains enriched with CAV1β compared to the other experimental conditions tested (CCPs or outside). Reduction of caveolae by downregulation via siRNA for CAV1 led to a significant reduction in the force of BMP2 binding and number of binding events demonstrating the importance of these regions in BMP2 binding. Downregulation of the BMP2 receptor BMPRIa by siRNA resulted in a significant decrease in the number of binding events demonstrating that our data was dependent upon BMP2 binding specifically to BMPRIa, not non-specific binding with the cell surface or other receptors. BMP2 does binds with high affinity to BMP type I receptors compared to BMP type II receptors (Koenig et al., 1994; Liu et al., 1995). Further the BMP type I receptor, BMBRIb, mRNA was not found in C2C12 cells (Mukai et al., 2007; Zilberberg et al., 2007). The data demonstrated for the first time that BMP2 receptors were housed in distinct environments on the plasma membrane and capable of binding to BMP2 with varying forces.

Downstream of BMP2 binding is BMPRIa phosphorylation by BMPRII and subsequently activation of BMP2 signaling. Downstream is the Smad pathway which regulates the genetic response. The sucrose density gradients showed the appearance of phosphorylated BMPRIa in caveolae therefore the initiation for BMP2 signaling is transduced in caveolae. Although phosphorylated BMPRIa was found to be in more dense fractions these include the Golgi, ER, CCPs, and early endosomes. Interestingly, BMPRIa was slightly phosphorylated in the absence of BMP2. This could be due to low levels of activated BMPRIa resulting in basal signaling or inhibitory phosphorylation, since these cells were serum starved resulting in cell cycle arrest. This phosphorylation also may be due to CK2 which is known to interact with BMPRIa in the absence of BMP2 (Bragdon et al., 2010). Further, the genetic response of BMP2-induced Smad pathway was decreased when caveolae were knocked down by siRNA against CAV1 or disrupted by Nystatin, demonstrating importance of caveolae in Smad signaling. Fascinatingly, treatment with Nystatin decreased Smad signaling to a different extent than the knockdown of CAV1. The Smad signal with the nystatin treatment was approximately a third of the BMP2 induced Smad signal. Work by Shi et al 2007 showed that 20–30% of the Smad pathway is decreased when the clathrin coated pit contribution to Smad signaling was decreased by knockdown of Endofin (an anchoring protein for Smad to clathrin coated pit endocytosis) (Shi et al., 2007). This indicates that CCPs are indeed areas for Smad signaling, but approximately 30%. This is similar to the response seen with the nystatin treatment, and within the error of the experiment.

The current model for BMP2 signaling must be extended to include the specific role of membrane domains in the initiation of Smad signaling (Bragdon et al., 2009; Hartung et al., 2006; Nohe et al., 2005; Rauch et al., 2002). Based on our data and previously published work, we suggest a new model for BMP signaling. Figure 8 shows the previous model for the activation of BMP2-induced Smad signaling. In this model BMPRIa and BMPRII are

localized in caveolae and CCPs. BMP2 binding initiates Smad signaling in CCPs and Smad dependent gene activation is dependent on endocytosis through CCPs (Hartung et al., 2006). On the other hand BMP2 binding to receptors housed in caveolae are responsible solely for the Smad independent signaling. Using our data and published recent literature, we suggest an extension of this model indicating that Smad signaling is additionally activated in caveolae and that BMP2 binds with a higher force and higher frequency to receptors localized in these domains.

Supplementary Material

Refer to Web version on PubMed Central for supplementary material.

Acknowledgments

We would like to express our sincere appreciation to Dr. Deni Galileo for the use of his ultracentrifuge, and Dr. Robert Gundersen for his helpful suggestions with sucrose gradients. We would like to acknowledge Joyita Dutta, Hemanth Akkiraju, and Rachel Schaefer for their support in the lab and suggestions.

Grants:

Contract Grant Sponsor: UDRF	Contract Grant Number: N/A
Contract Grant Sponsor: National Institute of Health	Contract Grant Number: RO1 AR043618
Contract Grant Sponsor: Startup University of Delaware	Contract Grant Number: N/A

References

Bragdon B, Moseychuk O, Saldanha S, King D, Julian J, Nohe A. Bone morphogenetic proteins: a critical review. Cell Signal. 2011; 23(4):609–620. [PubMed: 20959140]

Bragdon B, Thinakaran S, Bonor J, Underhill TM, Petersen NO, Nohe A. FRET reveals novel protein-receptor interaction of bone morphogenetic proteins receptors and adaptor protein 2 at the cell surface. Biophys J. 2009; 97(5):1428–1435. [PubMed: 19720031]

Bragdon B, Thinakaran S, Moseychuk O, King D, Young K, Litchfield DW, Petersen NO, Nohe A. Casein kinase 2 beta-subunit is a regulator of bone morphogenetic protein 2 signaling. Biophys J. 2010; 99(3):897–904. [PubMed: 20682268]

Buckle, H. American Society for Metals. Materials Park, Ohio: 1973. The science of hardness testing and its research applications.

Cai T, Wang H, Chen Y, Liu L, Gunning WT, Quintas LE, Xie ZJ. Regulation of caveolin-1 membrane trafficking by the Na/K-ATPase. J Cell Biol. 2008; 182(6):1153–1169. [PubMed: 18794328]

Chen YG, Wang Z, Ma J, Zhang L, Lu Z. Endofin, a FYVE domain protein, interacts with Smad4 and facilitates transforming growth factor-beta signaling. J Biol Chem. 2007; 282(13):9688–9695. [PubMed: 17272273]

Doak SH, Rogers D, Jones B, Francis L, Conlan RS, Wright C. High-resolution imaging using a novel atomic force microscope and confocal laser scanning microscope hybrid instrument: essential sample preparation aspects. Histochem Cell Biol. 2008; 130(5):909–916. [PubMed: 18719934]

Fujimoto T, Kogo H, Nomura R, Une T. Isoforms of caveolin-1 and caveolar structure. J Cell Sci. 2000; 113(Pt 19):3509–3517. [PubMed: 10984441]

Gamell C, Osses N, Bartrons R, Ruckle T, Camps M, Rosa JL, Ventura F. BMP2 induction of actin cytoskeleton reorganization and cell migration requires PI3-kinase and Cdc42 activity. J Cell Sci. 2008; 121(Pt 23):3960–3970. [PubMed: 19001503]

Hartung A, Bitton-Worms K, Rechtman MM, Wenzel V, Boergermann JH, Hassel S, Henis YI, Knaus P. Different routes of bone morphogenic protein (BMP) receptor endocytosis influence BMP signaling. Mol Cell Biol. 2006; 26(20):7791–7805. [PubMed: 16923969]

Haupt BJ, Pelling AE, Horton MA. Integrated confocal and scanning probe microscopy for biomedical research. Scientific World Journal. 2006; 6:1609–1618. [PubMed: 17173179]

Ide H, Saito-Ohara F, Ohnami S, Osada Y, Ikeuchi T, Yoshida T, Terada M. Assignment of the BMPR1A and BMPR1B genes to human chromosome 10q22.3 and 4q23-->q24 byin situ hybridization and radiation hybrid map ping. Cytogenet Cell Genet. 1998; 81(3–4):285–286. [PubMed: 9730621]

Itoh S, Itoh F, Goumans MJ, Ten Dijke P. Signaling of transforming growth factor-beta family members through Smad proteins. Eur J Biochem. 2000; 267(24):6954–6967. [PubMed: 11106403]

Jiang Y, Nohe A, Bragdon B, Tian C, Rudarakanchana N, Morrell NW, Petersen NO. Trapping of BMP receptors in distinct membrane domains inhibiti their function in pulmonary arterial hypertension. American Journal of Physiology - Lung Cellular and Molecular Physiology. 2011

Keating E, Nohe A, Petersen NO. Studies of distribution, location and dynamic properties of EGFR on the cell surface measured by image correlation spectroscopy. Eur Biophys J. 2008; 37(4):469–481. [PubMed: 18043914]

Koenig BB, Cook JS, Wolsing DH, Ting J, Tiesman JP, Correa PE, Olson CA, Pecquet AL, Ventura F, Grant RA, et al. Characterization and cloning of a receptor for BMP-2 and BMP-4 from NIH 3T3 cells. Mol Cell Biol. 1994; 14(9):5961–5974. [PubMed: 8065329]

Kogo H, Fujimoto T. Caveolin-1 isoforms are encoded by distinct mRNAs. Identification Of mouse caveolin-1 mRNA variants caused by alternative transcription initiation and splicing. FEBS Lett. 2000; 465(2–3):119–123. [PubMed: 10631317]

Liu F, Ventura F, Doody J, Massague J. Human type II receptor for bone morphogenic proteins (BMPs): extension of the two-kinase receptor model to the BMPs. Mol Cell Biol. 1995; 15(7): 3479–3486. [PubMed: 7791754]

Matveev S, Li X, Everson W, Smart EJ. The role of caveolae and caveolin in vesicle-dependent and vesicle-independent trafficking. Adv Drug Deliv Rev. 2001; 49(3):237–250. [PubMed: 11551397]

McNiven MA. Dynamin: a molecular motor with pinchase action. Cell. 1998; 94(2):151–154. [PubMed: 9695943]

Mellman I. Endocytosis and molecular sorting. Annu Rev Cell Dev Biol. 1996; 12:575–625. [PubMed: 8970738]

Mukai T, Otsuka F, Otani H, Yamashita M, Takasugi K, Inagaki K, Yamamura M, Makino H. TNF-alpha inhibits BMP-induced osteoblast differentiation through activating SAPK/JNK signaling. Biochem Biophys Res Commun. 2007; 356(4):1004–1010. [PubMed: 17397798]

Muller DJ, Helenius J, Alsteens D, Dufrene YF. Force probing surfaces of living cells to molecular resolution. Nat Chem Biol. 2009; 5(6):383–390. [PubMed: 19448607]

Murphy C. Endo-fin-ally a SARA for BMP receptors. J Cell Sci. 2007; 120(Pt 7):1153–1155. [PubMed: 17376961]

Nohe A, Keating E, Loh C, Underhill MT, Petersen NO. Caveolin-1 isoform reorganization studied by image correlation spectroscopy. Faraday Discuss. 2004; 126:185–195. discussion 245-154. [PubMed: 14992406]

Nohe A, Keating E, Underhill TM, Knaus P, Petersen NO. Effect of the distribution and clustering of the type I A BMP receptor (ALK3) with the type II BMP receptor on the activation of signalling pathways. J Cell Sci. 2003; 116(Pt 16):3277–3284. [PubMed: 12829744]

Nohe A, Keating E, Underhill TM, Knaus P, Petersen NO. Dynamics and interaction of caveolin-1 isoforms with BMP-receptors. J Cell Sci. 2005; 118(Pt 3):643–650. [PubMed: 15657086]

Pachori AS, Custer L, Hansen D, Clapp S, Kemppa E, Klingensmith J. Bone morphogenetic protein 4 mediates myocardial ischemic injury through JNK-dependent signaling pathway. J Mol Cell Cardiol. 2010; 48(6):1255–1265. [PubMed: 20096288]

Persch G, Born C, Utesch B. Nano-harness investigations of thin fils by atomic force microscope. Microelectronic Engineering. 1994; 24(1–4):113–121.

Ramirez MI, Pollack L, Millien G, Cao YX, Hinds A, Williams MC. The alpha-isoform of caveolin-1 is a marker of vasculogenesis in early lung development. J Histochem Cytochem. 2002; 50(1):33–42. [PubMed: 11748292]

Ramos M, Lame MW, Segall HJ, Wilson DW. The BMP type II receptor is located in lipid rafts, including caveolae, of pulmonary endothelium in vivo and in vitro. Vascul Pharmacol. 2006; 44(1):50–59. [PubMed: 16271518]

Rauch C, Brunet AC, Deleule J, Farge E. C2C12 myoblast/osteoblast transdifferentiation steps enhanced by epigenetic inhibition of BMP2 endocytosis. Am J Physiol Cell Physiol. 2002; 283(1):C235–C243. [PubMed: 12055092]

Reilly GC, Golden EB, Grasso-Knight G, Leboy PS. Differential effects of ERK and p38 signaling in BMP-2 stimulated hypertrophy of cultured chick sternal chondrocytes. Cell Commun Signal. 2005; 3(1):3. [PubMed: 15691373]

Schmid SL. Clathrin-coated vesicle formation and protein sorting: an integrated process. Annu Rev Biochem. 1997; 66:511–548. [PubMed: 9242916]

Shi W, Chang C, Nie S, Xie S, Wan M, Cao X. Endofin acts as a Smad anchor for receptor activation in BMP signaling. J Cell Sci. 2007; 120(Pt 7):1216–1224. [PubMed: 17356069]

Shin JS, Gao Z, Abraham SN. Involvement of cellular caveolae in bacterial entry into mast cells. Science. 2000; 289(5480):785–788. [PubMed: 10926542]

Sieber C, Kopf J, Hiepen C, Knaus P. Recent advances in BMP receptor signaling. Cytokine Growth Factor Rev. 2009; 20(5–6):343–355. [PubMed: 19897402]

Song KS, Li S, Okamoto T, Quilliam LA, Sargiacomo M, Lisanti MP. Co-purification and direct interaction of Ras with caveolin, an integral membrane protein of caveolae microdomains. Detergent-free purification of caveolae microdomains. J Biol Chem. 1996; 271(16):9690–9697. [PubMed: 8621645]

Wertz JW, Bauer PM. Caveolin-1 regulates BMPRII localization and signaling in vascular smooth muscle cells. Biochem Biophys Res Commun. 2008; 375(4):557–561. [PubMed: 18725205]

Yamashita H, Ten Dijke P, Heldin CH, Miyazono K. Bone morphogenetic protein receptors. Bone. 1996; 19(6):569–574. [PubMed: 8968021]

Yanai I, Benjamin H, Shmoish M, Chalifa-Caspi V, Shklar M, Ophir R, Bar-Even A, Horn-Saban S, Safran M, Domany E, Lancet D, Shmueli O. Genome-wide midrange transcription profiles reveal expression level relationships in human tissue specification. Bioinformatics. 2005; 21(5):650–659. [PubMed: 15388519]

Zilberberg L, ten Dijke P, Sakai LY, Rifkin DB. A rapid and sensitive bioassay to measure bone morphogenetic protein activity. BMC Cell Biol. 2007; 8:41. [PubMed: 17880711]

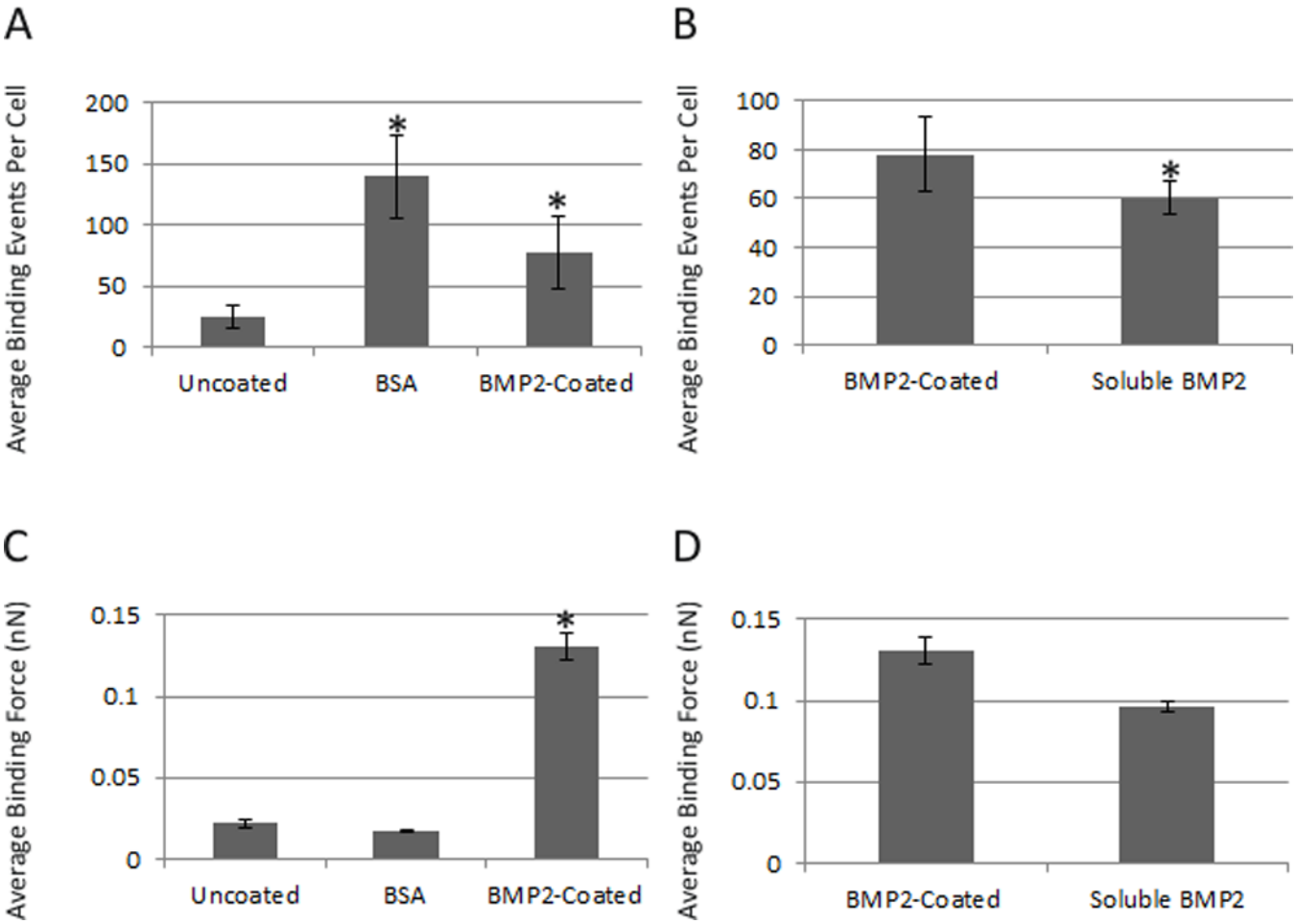

Figure 1.

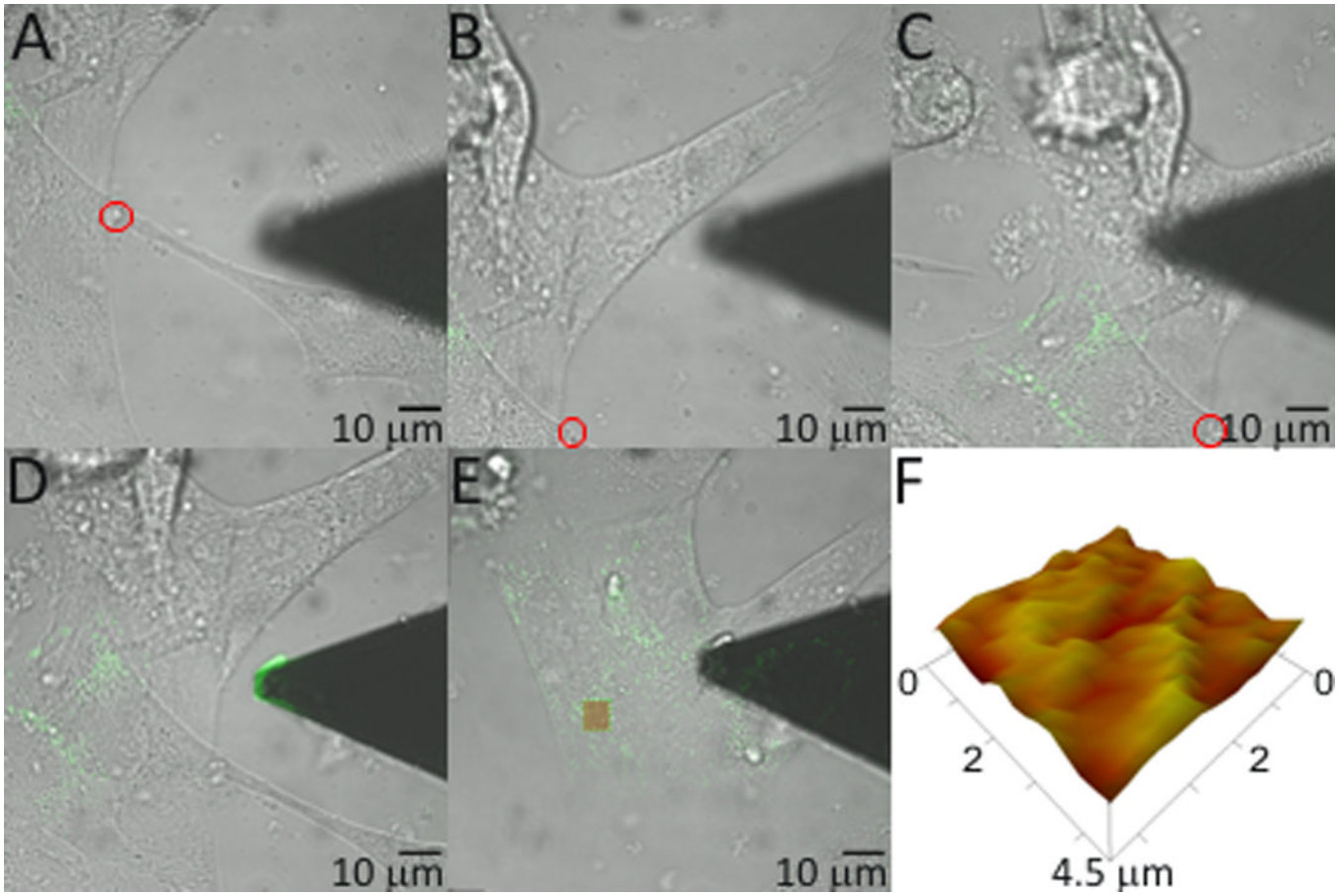

Figure 2.

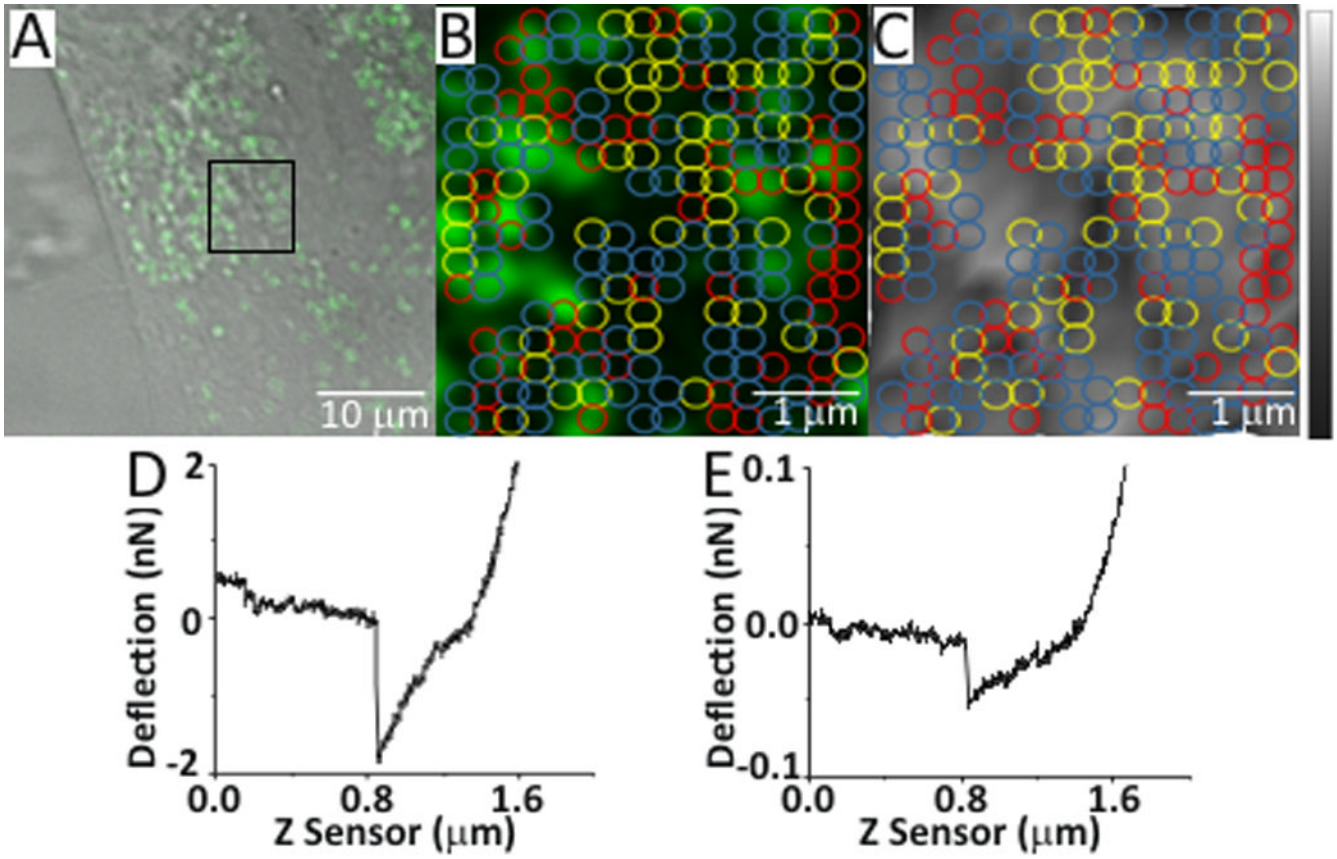

Figure 3.

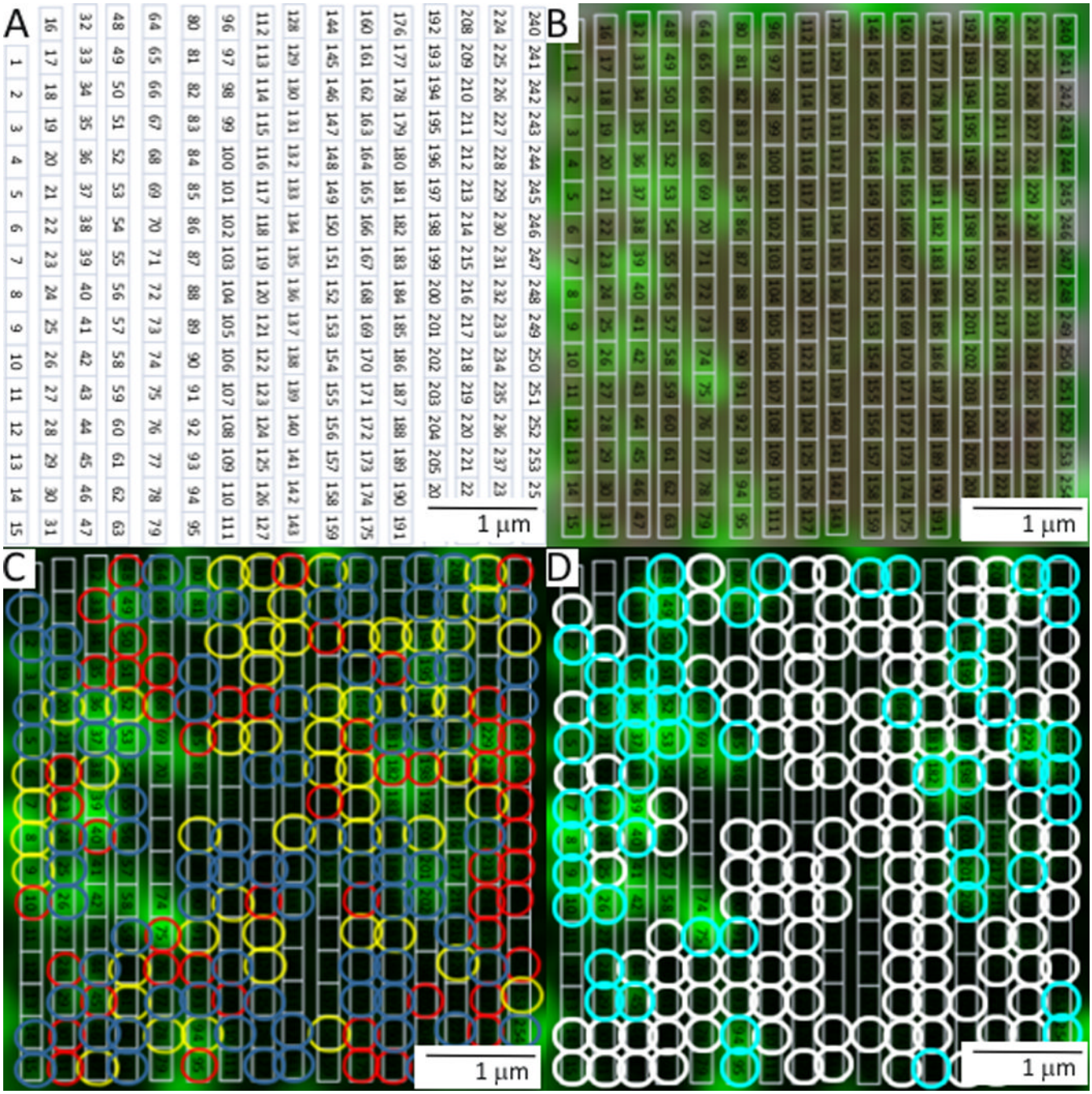

Figure 4.

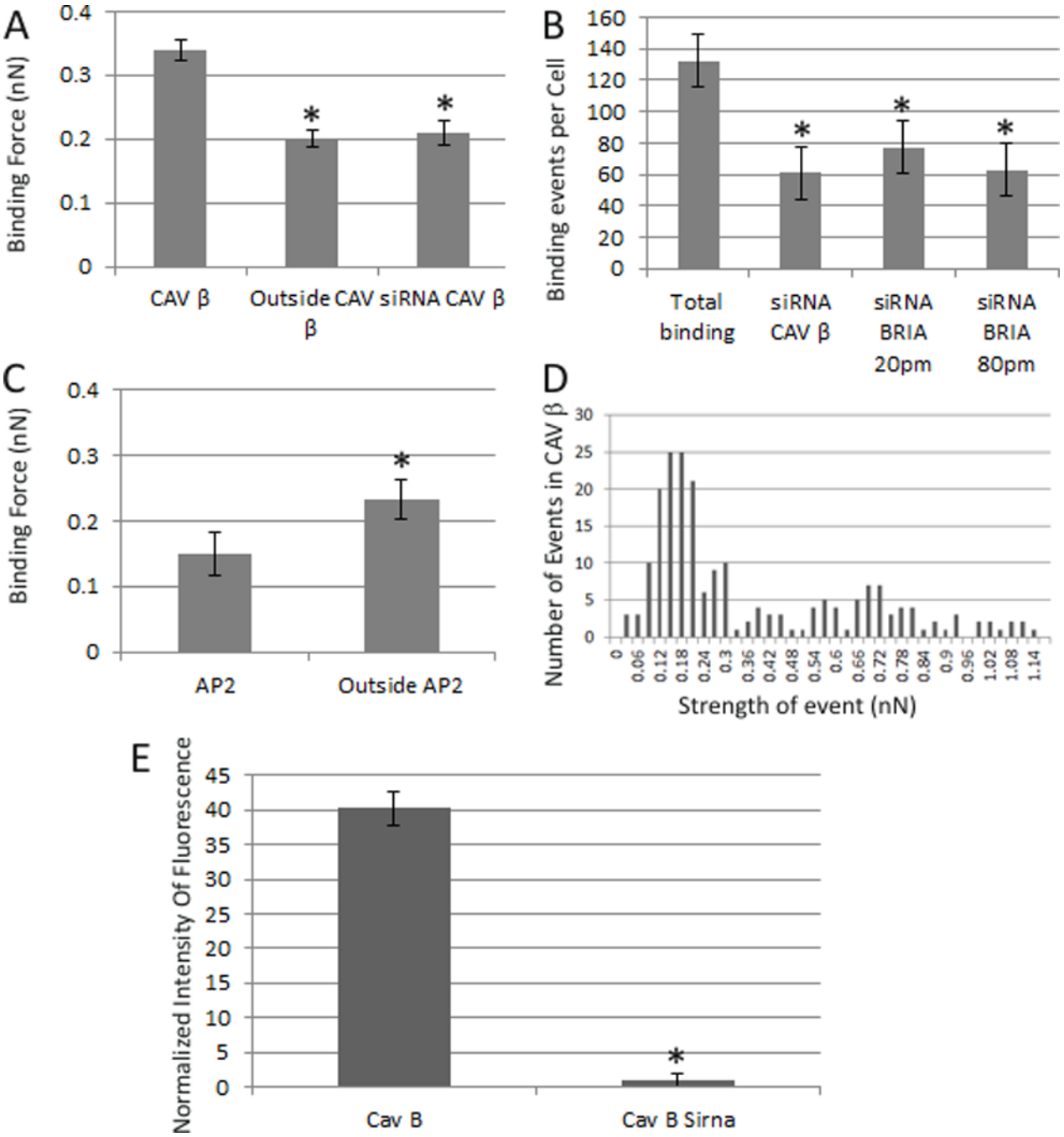

Figure 5.

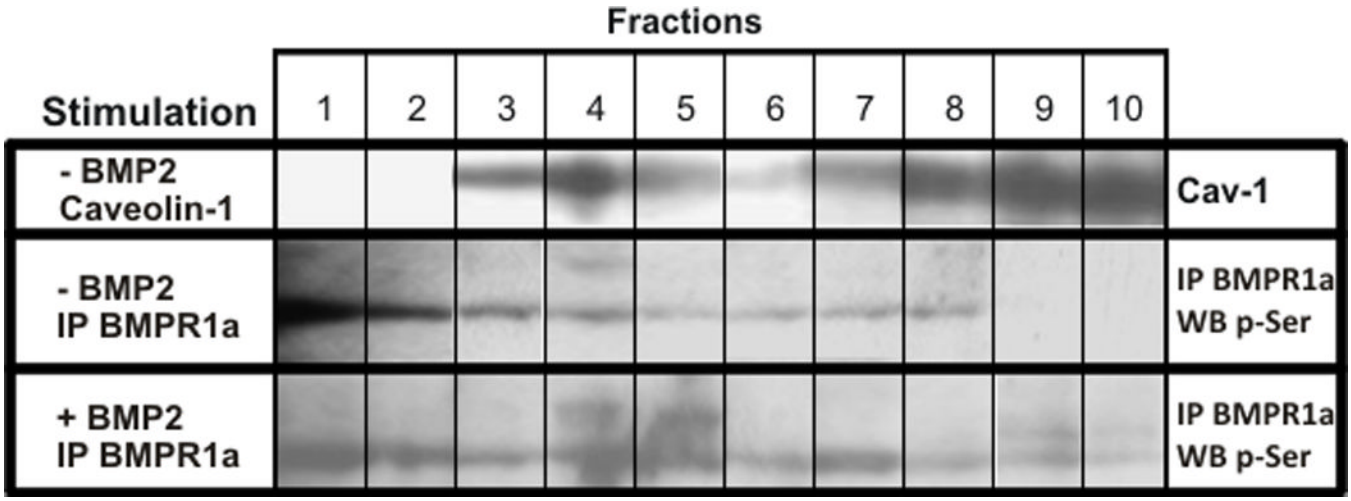

Figure 6.

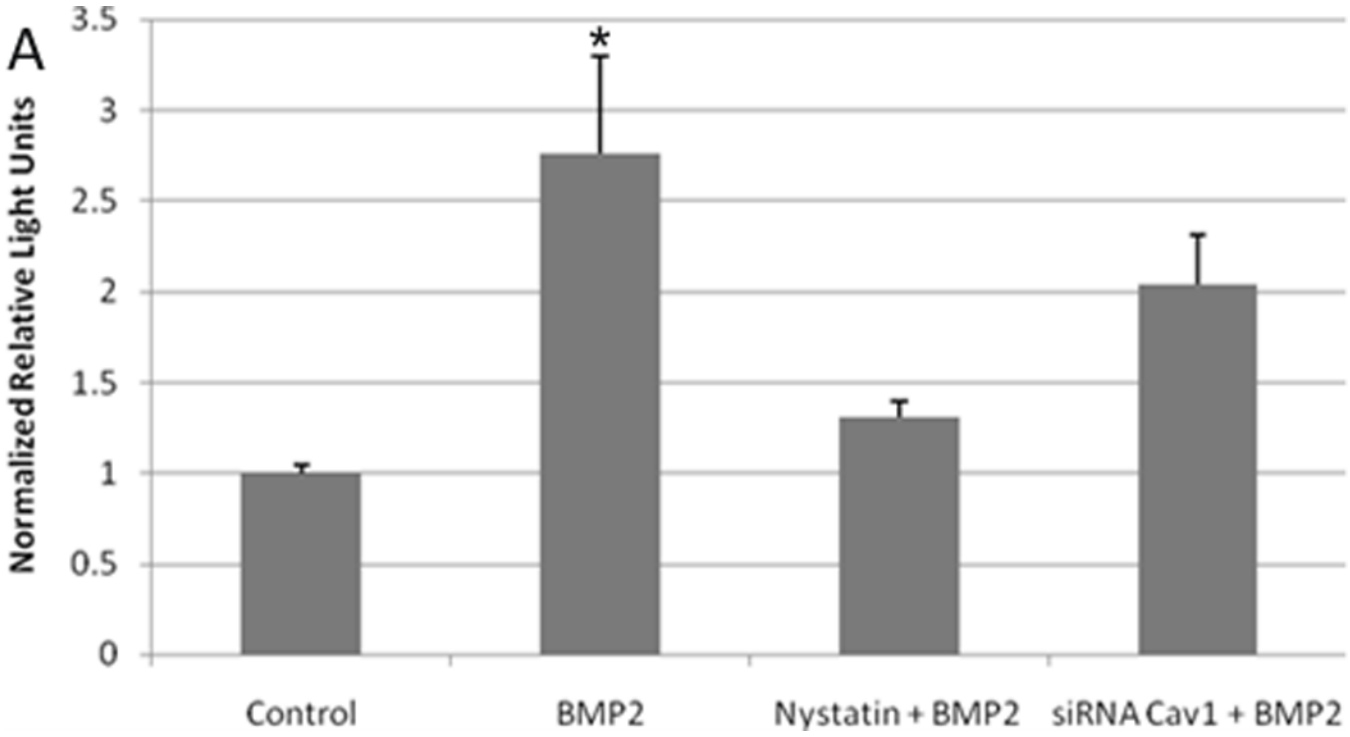

Figure 7.

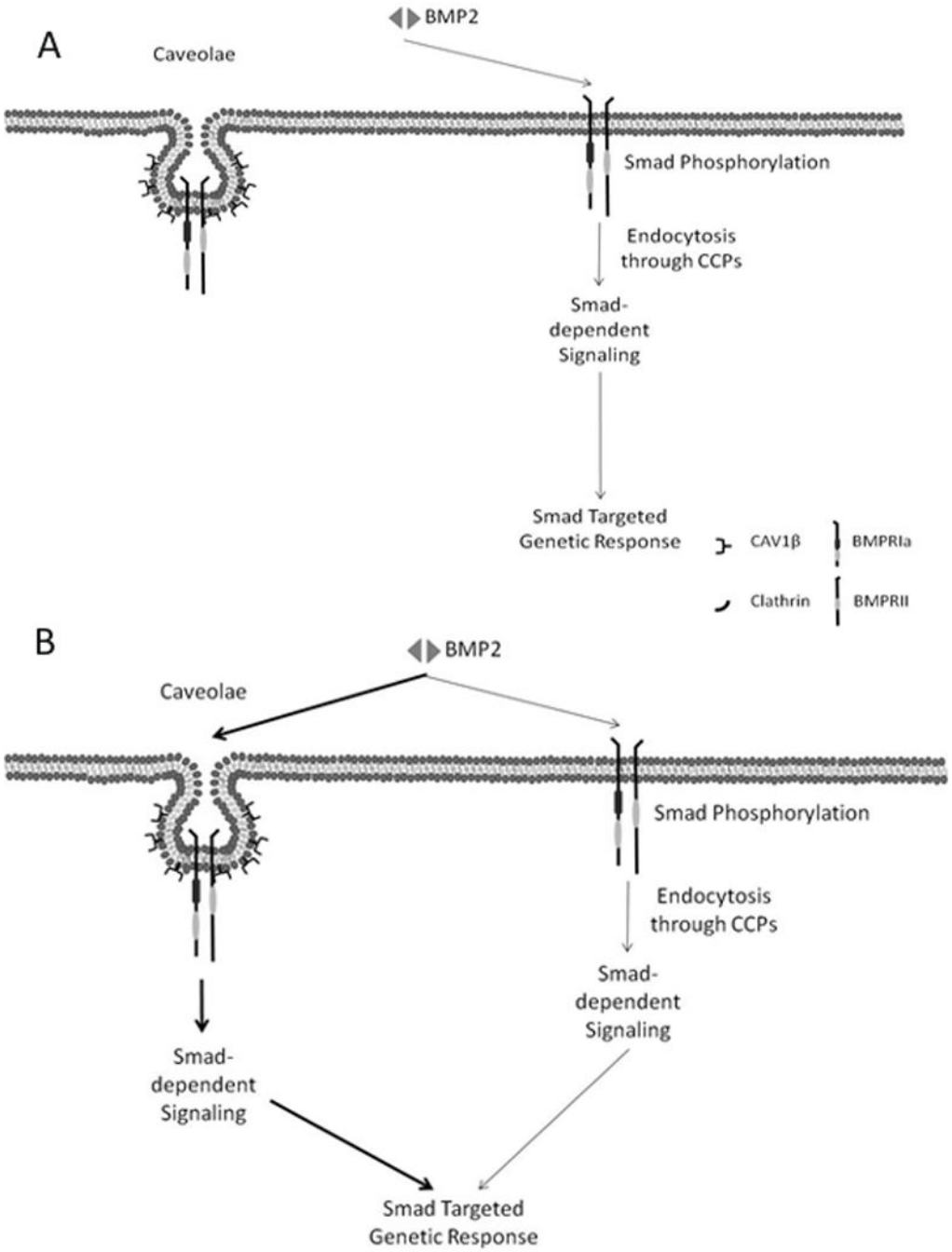

Figure 8.